0026-895X/08/7303-697–708$20.00
MOLECULAR PHARMACOLOGY
Vol. 73, No. 3
40931/3304546
Mol Pharmacol 73:697–708, 2008
Printed in U.S.A.

Derlin-1 and p97/Valosin-Containing Protein Mediate the Endoplasmic Reticulum-Associated Degradation of Human V2 Vasopressin Receptors[S]

Isabel Schwieger, Katja Lautz, Eberhard Krause, Walter Rosenthal, Burkhard Wiesner, and Ricardo Hermosilla

Charité-Universitätsmedizin Berlin, Bereich Molekulare Pharmakologie und Zellbiologie, Berlin, Germany

Received August 15, 2007; accepted November 26, 2007

ABSTRACT

The endoplasmic reticulum-associated degradation (ERAD), the main quality control pathway of the cell, is crucial for the elimination of unfolded or misfolded proteins. Several diseases are associated with the retention of misfolded proteins in the early secretory pathway. Among them is X-linked nephrogenic diabetes insipidus, caused by mutations in the gene encoding the V2 vasopressin receptor (V2R). We studied the degradation pathways of three intracellularly retained V2R mutants with different misfolded domains in human embryonic kidney 293 cells. At steady state, the wild-type V2R and the complex-glycosylated mutant G201D were partially located in lysosomes, whereas core-glycosylated mutants L62P and V226E were excluded from this compartment. In pulse-chase experiments, proteasomal inhibition stabilized the nonglycosylated and core-glycosylated forms of all studied receptors. In addition, all mutants and the wild-type receptor were found to be polyubiquitinylated. Nonglycosylated and core-glycosylated receptor forms were located in cytosolic and membrane fractions, respectively, confirming the deglycosylation and retrotranslocation of ERAD substrates to the cytosol. Distinct Derlin-1-dependent and -independent ERAD pathways have been proposed for proteins with different misfolded domains (cytosolic, extracellular, and membrane) in yeast. Here, we show for the first time that V2R mutants with different misfolded domains are able to coprecipitate the ERAD components p97/valosin-containing protein, Derlin-1 and the 26S proteasome regulatory subunit 7. Our results demonstrate the presence of a Derlin-1-mediated ERAD pathway degrading wild-type and disease-causing V2R mutants with different misfolded domains in a mammalian system.

Several human diseases are caused by the retention or accumulation of a protein within the cell. The quality control system of the secretory pathway screens for non-native protein conformations (e.g., unfolded or misfolded proteins), impedes their further transport, and targets them to the degradation system. These proteins do not reach their site of action, which leads to a loss of function and thereby to disease (Aridor and Hannan, 2000; Aridor and Hannan, 2002). In general, there are two fates for these retained proteins: either they are degraded or they accumulate. Protein accumulation in the endoplasmic reticulum (ER) may lead to an unfolded protein response, ER overload response, or both (Zhang and Kaufman, 2006). Other proteins may accumulate in the cytosol, which eventually leads to the formation of intracellular aggregates or aggresomes (Kopito, 2000), but ultimately, in both cases, the cell is damaged and apoptosis is induced.

The intracellular retention of the V2 vasopressin receptor (V2R) causes X-linked nephrogenic diabetes insipidus (NDI). More than 170 different mutations of the *AVPR2* gene, each of them causing NDI, have been described in the literature

This work was supported by Deutsche Forschungsgemeinschaft grants DFG HE4468-1/1 and -1/2.
Article, publication date, and citation information can be found at http://molpharm.aspetjournals.org.
doi:10.1124/mol.107.040931.
[S] The online version of this article (available at http://molpharm.aspetjournals.org) contains supplemental material.

ABBREVIATIONS: ER, endoplasmic reticulum; V2R, human V2 vasopressin receptor; NDI, nephrogenic diabetes insipidus; AVP, 8-arginine vasopressin; ERGIC, ER/Golgi intermediate compartment; ERAD, endoplasmic reticulum-associated degradation (-C, -L, and -M, misfolded cytosolic, luminal, and intramembrane domain, respectively); p97/VCP, valosin-containing protein; GPCR, G protein-coupled receptor; Der, Derlin; HEK, human embryonic kidney; PMSF, phenylmethylsulfonyl fluoride; STI, soybean trypsin inhibitor; POD, horseradish peroxidase; GAPDH, glyceraldehyde-3-phosphate dehydrogenase; MG 132, *N*-benzoyloxycarbonyl (*Z*)-Leu-Leu-leucinal; GFP, green fluorescent protein; DMEM, Dulbecco's modified Eagle's medium; PBS, phosphate-buffered saline; PAGE, polyacrylamide gel electrophoresis; RT, room temperature; ECL, enhanced chemiluminescence; MS/MS, tandem mass spectrometry; HSP, heat shock protein; Rpt1/S7, 26S protease regulatory subunit 7; Rpn1/S2, proteasome 26S non-ATPase subunit 2; Rpn10/S5a, 26S protease regulatory subunit 5a; RP, regulatory particle.

(http://www.medicine.mcgill.ca/nephros). The V2R is normally expressed at the plasma membrane of renal epithelial cells of the collecting duct, and it regulates vasopressin (AVP)-mediated water reabsorption in the kidney. The majority of NDI-causing mutations produce receptors that are retained in different intracellular compartments, such as the ER, ER/Golgi intermediate compartment (ERGIC) (Hermosilla et al., 2004), and Golgi apparatus. A few NDI-causing mutants are expressed at the cell surface, but they fail to get activated by AVP (Robben et al., 2006). Patients with NDI suffer from polyuria, polydipsia, nocturia, and failure to thrive.

Disease-causing V2R mutants that are retained in different compartments of the secretory pathway are good models to elucidate the interactions between the quality control system and degradation pathways. Intracellular degradation of membrane proteins is carried out by lysosomes, the ubiquitin/proteasome system, or both, depending on the intracellular localization of the protein. Proteins localized at the plasma membrane are usually degraded in lysosomes, such as the wild-type V2R (Bouley et al., 2005). ER-retained proteins are targeted to the ER-associated degradation (ERAD) pathway. ER-retained misfolded membrane proteins are polyubiquitinylated by ubiquitin ligases (gp78 and Hrd1), and they are pulled out of the ER membrane by AAA-ATPases [p97/valosin-containing protein (p97/VCP)] and ATPases of the 19S proteasome (Meusser et al., 2005; Wahlman et al., 2007) through channel proteins, such as Sec61α, Derlin-1, -2, or -3, or a combination. They are deglycosylated, deubiquitinylated, and unfolded before being degraded by the 26S proteasome (Werner et al., 1996; Hampton, 2002). G protein-coupled receptors (GPCR), as the δ opioid receptor, luteinizing hormone receptor, and some disease-causing V2R mutants, have been associated with proteasomal degradation in mammalian cells (Petäjä-Repo et al., 2001; Pietilä et al., 2005; Robben et al., 2005); however, their degradation mechanisms are not fully understood. Furthermore, how receptor proteins are degraded that are neither retained in the ER nor localized at the cell membrane, such as V2R mutants that are retained in the ERGIC (V226E) and Golgi apparatus (G201D), remains unknown.

In yeast, three distinct ERAD pathways (ERAD-L for misfolded ER-luminal domains; ERAD-M, for misfolded intramembrane domains; and ERAD-C, for misfolded cytosolic domains of substrate proteins) have been proposed previously (Carvalho et al., 2006). ERAD-L and ERAD-M require the ubiquitin ligase Hrd1 and its cofactor Hrd3, but not Doa10 as in the ERAD-C pathway. Der1 (Derlin-1, -2, and -3 in mammals) is required in the ERAD-L pathway. All ERAD pathways require the ATPase complex of Ubx2, Npl4, Ufd1, and Cdc48 (p97/VCP in mammals). So far, it is unknown whether these distinct pathways also operate in mammalian cells. In the present work, we analyzed the degradation pathways of the wild-type V2R and of three NDI-causing V2R mutants with misfolded cytosolic (L62P), luminal (G201D), and intramembrane (V226E) domains that are retained in different intracellular compartments, namely, the ER, ERGIC, and Golgi apparatus, respectively. The wild-type receptor and all intracellular retained mutants are polyubiquitinylated and interact with the ERAD components Derlin-1, the AAA-ATPase p97/VCP, and the 26S proteasome regulatory subunit 7 (Rpt1/S7), regardless of the location of their misfolded domains. Our results show that substrates with different misfolded domains are degraded by a Derlin-1, p97/VCP-mediated ERAD pathway in HEK923 cells.

Materials and Methods

Materials. [^{3}H]cAMP (0.925 TBq/mmol), [α-^{32}P]ATP (29.6 TBq/mmol), and [^{35}S]EasyTag protein labeling mix (43.48 TBq/mmol) were obtained from PerkinElmer Life and Analytical Sciences (Boston, MA). Lipofectamine 2000 was purchased from Invitrogen (Karlsruhe, Germany), and FuGENE 6 was from Roche Diagnostics (Mannheim, Germany). Restriction enzymes were from New England Biolabs (Schwalbach, Germany). Trypsin (sequencing grade) was obtained from Promega (Madison, WI). PMSF, deoxycholic acid sodium salt, Roti-Load 1, and SDS were from Roth (Karlsruhe, Germany). Dulbecco's modified Eagle's medium (without methionine and cysteine), benzamidine, chloroquine diphosphate salt, protein A-Sepharose, protein G-agarose, rabbit polyclonal α-Derlin-1 antibody, mouse monoclonal α-actin antibody, rabbit polyclonal α-FLAG antibody, mouse monoclonal α-FLAG M2 antibody, and α-FLAG M2 affinity gel were from Sigma (Munich, Germany). Aprotinin (Trasylol), Tween 20, trypsin inhibitor (STI), and the chemiluminescence detection kit for horseradish peroxidase (POD) were from Applichem (Darmstadt, Germany). The POD-conjugated goat α-rabbit and goat α-mouse antibodies were purchased from Dianova (Hamburg, Germany). The rabbit α-p97/VCP antibody and the monoclonal rabbit α-GAPDH antibody were from Cell Signaling Technology Inc. (Danvers, MA). The rabbit α-19S proteasome subunit Rpt1 antibody was from Biomol GmbH (Hamburg, Germany). The rabbit α-calnexin antibody and the monoclonal mouse anti-multiubiquitin antibody were from Assay Designs, Inc. (Ann Arbor, MI). The polyclonal goat α-Derlin-1 antibody was from Santa Cruz Biotechnology, Inc. (Santa Cruz, CA). LysoTracker Red was from Invitrogen. MG 132 was purchased from Calbiochem (Darmstadt, Germany). Plasmid pV2R.DNA3.1, coding for the untagged V2R, and plasmid pEU367.GFP, encoding a C-terminally green fluorescent protein (GFP)-tagged V2R, have been described previously (Oksche et al., 1998; Schülein et al., 1998). The pEGFP-N1 vector was from Clontech Laboratories (Heidelberg, Germany). The QuikChange site-directed mutagenesis kit was purchased from Stratagene (La Jolla, CA), and the Qproteome cell compartment kit was from QIAGEN GmbH (Hilden, Germany). HEK293 cells were purchased from DSMZ (Hannover, Germany).

Plasmid Constructions. Plasmid pFLAG.V2R encoding the V2R with a FLAG tag fused to the N terminus was made via polymerase chain reaction with a BamHI/FLAG insertion primer (5′-CGGGATCCCGGCCACCATGGA-CTATAAGGACGATGACGATAAGATGCTCATGGCGTCCACTTCCGC-3′) and the commercially available pcDNA3.1/BGH reverse sequencing primer from Invitrogen. For this reaction, pV2R.DNA3.1 was used as a template. The polymerase chain reaction product, containing the FLAG.V2R cDNA and an N-terminally inserted BamHI site, was cloned into the pcDNA3.1 vector using the introduced BamHI site and XbaI site. Plasmids pFLAG.L62P, pFLAG.V226E, and pFLAG.G201D were constructed with the help of the QuikChange site-directed mutagenesis kit (Stratagene; primer sequences available on request); plasmid pFLAG.V2R was used as template. Plasmids pL62P.GFP, pV226E.GFP, and pG201D.GFP encoding the receptor mutants L62P, V226E, and G201D, tagged with GFP at their C termini (residue Lys367), have been described previously (Krause et al., 2000). Standard DNA preparations and cloning techniques were carried out according to the handbooks of Sambrook and Russell (2001). The nucleotide sequences of the DNA fragments were verified by sequencing, using the BigDye Terminator kit (Applied Biosystems).

Cell Culture. HEK293 cells were maintained in Dulbecco's modified Eagle's medium (DMEM) from Sigma, supplemented with 10% (v/v) heat-inactivated fetal bovine serum, 20 mM glutamine, 100 IU penicillin, and 100 μg/ml streptomycin in a 5% CO_2 atmosphere at 37°C. Stably expressing cell lines were generated through transfec-

tion with FuGENE 6 (Roche Diagnostics) or Lipofectamine 2000 (Invitrogen) according to the manufacturer's recommendations. Clones were selected with 400 μg/ml G-418 (Geneticin; Calbiochem). The culture medium for the stably expressing cell clones was additionally supplemented with 400 μg/ml G-418.

Adenylyl Cyclase Assay. The adenylyl cyclase assays were carried out with nuclei-free crude membranes of stably transfected HEK293 cells as described previously for stably transfected mouse Ltk$^-$ cells (Schülein et al., 1996).

Total Cell Lysis. HEK293 cells stably expressing V2R constructs were grown to confluence on a 60-mm culture dish. Cells were washed two times with ice-cold PBS, and then they were lysed in 500 μl of radioimmunoprecipitation assay buffer; the method has been described previously (Gazit et al., 1999). After determination of protein concentration, 30 μg of the total amount of proteins was used for SDS-PAGE.

Immunoprecipitation of FLAG-Tagged V2Rs and Coimmunoprecipitation. HEK293 cells stably expressing V2R constructs were grown to confluence on a 60-mm culture dish. Cells were washed two times with ice-cold PBS, lysed in 1 ml of ice-cold lysis buffer (1% Triton X-100, 0.1% SDS, 50 mM Tris-HCl, 150 mM NaCl, 1 mM Na-EDTA, 0.5 mM PMSF, 10 μg/ml STI, 1 μg/ml aprotinin, and 0.5 mM benzamidine, pH 8.0), and then transferred to microfuge tubes. The insoluble fraction of one 60-mm culture dish was removed by centrifugation (20 min; 4°C; 18,620*g*), and FLAG-tagged proteins were isolated from the supernatant with an immune complex of 5 mg of protein A-Sepharose beads and 5 μg of α-FLAG Sigma M2 antibodies at 4°C overnight. Beads were centrifuged (1 min; 4°C; 13,680*g*), and washed three times with buffer A (0.5% Triton X-100, 0.1% SDS, 50 mM Tris-HCl, 500 mM NaCl, 1 mM Na-EDTA, pH 8.0) and once with buffer B (0.5% Triton X-100, 0.1% SDS, 50 mM Tris-HCl, and 1 mM Na-EDTA, pH 7.4). Bound proteins were eluted by 5-min boiling (95°C) in 40 μl of 2× Roti-Load 1 sample buffer. They were separated by SDS-PAGE. For coimmunoprecipitation experiments, FLAG-tagged proteins were isolated with 40 μl of α-FLAG M2 Affinity gel (Sigma) (same preparation as described above) or with an immune complex of 5 mg of protein G-agarose beads and 2 μg of polyclonal α-Derlin-1 antibodies (Santa Cruz Biotechnology, Inc.) at 4°C overnight.

Immunoblots. Proteins were separated by SDS-PAGE (10 or 15% acrylamide), and then they were blotted onto nitrocellulose membranes as described previously (Kyhse-Andersen, 1984). Membranes were blocked for 1 h with PBS (140 mM NaCl, 2.7 mM KCl, and 10 mM KH_2PO_4, pH 7.4) supplemented with 0.1% Tween 20 and 5% low fat milk powder. For detection of the V2R, membranes were incubated with a mouse monoclonal α-FLAG M2 antibody (1:1500 in PBS with 0.1% Tween 20 and 2% low fat milk powder) for 1 h at RT. Membranes were washed three times (15 min each) with wash buffer (PBS supplemented with 0.1% Tween 20). Blots were incubated with a POD-conjugated α-mouse antibody (1:10,000) in PBS supplemented with 0.1% Tween 20 and 2% low fat milk powder for 45 min at RT. Membranes were washed again three times with wash buffer (15 min each). Finally, membranes were incubated in ECL system for 3 min, and they were developed with a luminescence X-Omat film (Eastman Kodak, Rochester, NY). For coimmunoprecipitation experiments, polyclonal α-p97/VCP antibody (Cell Signaling Technology Inc.), polyclonal rabbit α-Derlin-1 (Sigma), polyclonal α-19S regulator, ATPase subunit Rpt1 antibody (Biomol GmbH) (all at 1:1000 dilution), or mouse monoclonal α-FLAG M2 antibody (Sigma) (1:1500 dilution) was used.

Ubiquitinylation Assay. Stably transfected HEK293 cells were treated with 20 μM MG 132 in serum-free medium for 16 h. Lysis of cells expressing FLAG-tagged receptors was carried out, the insoluble fraction was removed by centrifugation (20 min; 4°C; 18,620*g*), and polyubiquitinylated proteins were isolated, as described in immunoprecipitation of FLAG-tagged V2Rs with 40 μl of α-FLAG M2 affinity gel (Sigma). After the washing steps, the proteins were boiled in 40 μl of 2× Roti-Load 1 sample buffer, separated by SDS-PAGE (10% acrylamide), and blotted onto nitrocellulose membranes. For detection, a mouse monoclonal anti-multiubiquitin antibody (Assay Design) (1:400) and a POD-conjugated α-mouse IgG (1:10,000) were used. The receptor expression was analyzed with a mouse monoclonal α-FLAG M2 antibody (Sigma) (1:1500) and a POD-conjugated α-mouse IgG (1:10,000). Immunoreactive bands were developed with ECL.

Visualization of GFP-Tagged Receptors by Confocal Laser-Scanning Microscopy in Living HEK293 Cells. Stably transfected HEK293 expressing the wild-type and mutant V2Rs tagged with GFP were grown for 24 to 48 h in a 35-mm culture dish containing a poly-L-lysine-coated coverslip. Cells were incubated with 150 nM LysoTracker Red for 1 h, and for inhibition of degradation, they were additionally incubated with 100 μM chloroquine for 3 h, washed once with PBS, and transferred immediately into a heating chamber (details on request). Cells were covered with 1 ml of PBS, and GFP fluorescence was visualized on a 510 inverted laser-scanning microscope (Carl Zeiss, Jena, Germany) (optical section: <0.9 μm; λ_{exc}, 488 nm; long pass filter, 505 nm). GFP and LysoTracker fluorescence signals were recorded (optical section: <0.9 μm; multitrack mode; GFP, λ_{exc}, 488 nm; band-pass filter, 494–548 nm; LysoTracker Red, λ_{exc}, 543 nm; long pass filter, 560 nm), and an overlay of both signals was computed.

Pulse-Chase Assay. Stably transfected HEK293 cells were grown in 100-mm culture dishes until confluence. Cells were starved in 5 ml of serum-free DMEM without methionine and cysteine (Sigma) for 16 h. The cells were washed twice with PBS, treated with trypsin/EDTA, and collected in a 15-ml Falcon tube (Falcon; BD Biosciences Discovery Labware, Bedford, MA). Cells were washed with PBS two more times (5 min; RT; 1000*g*). Metabolic labeling with 220 μCi of [^{35}S]EasyTag protein labeling mix in 500 μl of medium lacking methionine and cysteine was performed for 45 min. The labeling process was stopped with 4 ml of DMEM supplemented with unlabeled methionine (2.3 mM) and cysteine (0.75 mM). To indicated times at which cells were resuspended, 1 ml of suspension was harvested for each sample; the sample was then mixed with 750 μl of ice-cold DMEM supplemented with protease inhibitors [0.5 mM PMSF, 10 μg/ml STI (trypsin inhibitor), 1 μg/ml aprotinin, and 0.5 mM benzamidine], collected by a centrifugation step (5 min; 4°C; 1000*g*), and lysed with 500 μl of ice-cold lysis buffer. The FLAG-tagged receptors were immunoprecipitated as described above. After separation by SDS-PAGE (10% acrylamide), the gels were dried and then exposed to X-ray film. Lysosomal and proteasomal activity was inhibited with 100 μM chloroquine and 40 μM MG 132, respectively, supplemented in all buffers from the labeling step until the end of the chase.

Protein Identification by Mass Spectrometry. Proteins of HEK293 cells treated with and without MG 132 were immunoprecipitated, prepared as described above, and subjected to SDS-PAGE. Sample preparation, in-gel digestion, peptide extraction, and spectra acquisition were performed as described previously (Czupalla et al., 2006). In brief, proteins were stained with Coomassie Blue, excised from the gel, and subjected to in-gel digestion by trypsin. NanoLC-MS/MS experiments were performed on a quadruple orthogonal acceleration time-of-flight mass spectrometer Q-Tof Ultima (Micromass, Manchester, UK). A Micromass CapLC liquid-chromatography system with a capillary column (PepMap C18; 3 μm; 150 mm × 75 μm i.d.; Dionex, Idstein, Germany) was used to deliver the peptide solution to the nanoelectrospray source (PicoTip spray capillaries; New Objective, Woburn, MA). For protein identification, data were acquired in a data-dependent mode (survey scanning) using one MS scan followed by MS/MS scans of the most abundant peak. The processed MS/MS spectra and MASCOT server version 1.9 (Matrix Science Ltd., London, UK) were used to search in-house against the SwissProt protein database (210906 and 234112 sequences).

Subcellular Fractionation. Proteins of different cellular compartments were obtained with the Qproteome cell compartment kit (QIAGEN GmbH). Cytosolic and membrane fractions were isolated according to the manufacturer's protocol. Equal amounts of proteins

were used for SDS-PAGE. The purity of the fractions was controlled by detection of calnexin and GAPDH, concurrently the proteins served as a loading control. Detection of receptor proteins was carried out with a monoclonal α-FLAG M2 antibody (Sigma) and a POD-conjugated α-mouse IgG. Immunoreactive bands were developed with the ECL system.

Results

Lysosomal Degradation of V2 Vasopressin Receptors. The degradation of intracellularly retained GPCRs has not been characterized in detail. The subject of the present study was the degradation pathway of three intracellularly retained V2R mutants, with misfolded domains located in different parts of the receptor. The L62P mutation is localized in the first intracellular domain at the interface to the first transmembrane domain; G201D lays in the second extracellular loop and V226E in the fifth transmembrane domain (Fig. 1A). Mutants L62P and V226E are deficient in their ability to stimulate the adenylyl cyclase; mutant G201D is partially deficient, thereby confirming their disease-causing nature (Fig. 1B). All mutants also show a different subcellular localization. The L62P mutant is found exclusively in the ER, the V226E mutant in the ER, and ERGIC and the G201D mutant localizes in the ER, ERGIC, Golgi apparatus, and partially at the plasma membrane (Hermosilla et al., 2004) (Fig. 2, Supplemental Fig. 2). We first determined whether lysosomes are involved in the degradation of all mutants. To this end, the presence of the mutants in lysosomes was assessed in living HEK293 cells by confocal laser-scanning microscopy. Cell clones stably expressing the V2R mutants tagged with GFP were stained with the fluorescent lysosome marker LysoTracker Red. GFP fluorescence signals were recorded on the green channel, and the LysoTracker Red signals were recorded on the red channel; overlays were computed. L62P and V226E were diffusely localized within the cell, excluding the nucleus (Fig. 2, left). LysoTracker Red signals were detected as intracellular vesicles, frequently nearby the nucleus (Fig. 2, middle) and no colocalization with GFP signals could be identified in overlays of mutants L62P and V226E (Fig. 2, right). Mutant G201D was detected in vesicular structures and at the plasma membrane. Colocalization with LysoTracker Red signals was observed (Fig. 2, right). GFP fluorescence signals from the wild-type V2R were localized predominantly at the plasma membrane and in vesicular structures, which also colocalized with LysoTracker Red signals.

To confirm these results, we inhibited lysosomal enzymes, which should lead to an increase in the colocalization between GFP fluorescence and LysoTracker Red signals. Stably transfected HEK293 cells were treated with 100 μM chloroquine for 3 h. Only in mutant G201D and the wild-type receptor were GFP fluorescence signals increased (Fig. 3, left and right). No change in the GFP fluorescence signals and colocalization status with lysosomes of mutant L62P and V226E could be observed. These results demonstrate that G201D and the wild-type V2R, which reach the Golgi apparatus and plasma membrane, are transported to the lysosomal compartment for degradation at steady state. In contrast, mutants L62P and V226E retained by the quality control system in the ER or ER/ERGIC are excluded from lysosomal degradation.

MG 132 Inhibits the Degradation of Immature Forms of All Mutants and the Wild-Type V2R. Mutants L62P and V226E were excluded from lysosomal degradation by their retention in the ER and ERGIC. Hence, their degradation should be carried out by the proteasome. Therefore, we studied the proteasomal and lysosomal degradation of all mutants and wild-type V2R in HEK293 cells stably expressing N-terminally FLAG-tagged V2R constructs (see Supplemental Material and Supplemental Fig. 1 for the pharmacological characterization). Pulse-chase metabolic labeling experiments were done in the presence of the lysosomal enzyme inhibitor chloroquine, the proteasomal inhibitor MG 132, and under control conditions (untreated). Immunoprecipitated proteins were identified by autoradiography. At 0 h, the wild-type V2R showed one prominent band at 38 kDa and another at 35 kDa, the first corresponding to the core-glycosylated (endoglycosydase H- and peptide endoglycosydase F-sensitive) and the second to the nonglycosylated receptor form (endoglycosydase H- and peptide endoglycosydase F-resistant; Supplemental Fig. 3) (Fig. 4, left). Both bands were present at 2.5 h of chase; additionally, a third broader band running between 55 and 45 kDa was noted. This band corresponds to the mature, complex-glycosylated form of the receptor (Supplemental Fig. 3). After 5 and 10 h of chase, the 35-kDa band became undetectable and only bands corresponding to the glycosylated receptor forms were present.

A similar band pattern was detected for mutant G201D. However, bands representing the complex-glycosylated receptor forms were less prominent. In contrast to the wild-type V2R and mutant G201D, mutants V226E and L62P showed two bands only, corresponding to immature forms of the receptor (nonglycosylated and core-glycosylated); complex-glycosylated forms were not detectable (Fig. 4, left, Supplemental Fig. 3). Under control conditions, the immature forms of mutants L62P and V226E persisted longer then that of mutant G201D and the wild-type receptor, indicating that the forward transport of the latter is also responsible for a signal reduction (Fig. 4, left).

Treatment with 100 μM chloroquine had no apparent effect on the band pattern of the wild-type V2R, indicating that its lysosomal degradation half-life is longer than 10 h. For mutant G201D, a change was only observed in the complex-glycosylated band, confirming that the mutant is degraded in lysosomes. Mutants V226E and L62P showed no change in their band pattern, demonstrating that they do not reach the lysosomal compartment.

In addition, cell clones were treated with the proteasomal inhibitor MG 132, and bands representing the nonglycosylated and core-glycosylated receptors (immature receptor forms) could be stabilized in all samples (Fig. 4, right). This result shows that proteasomal activity is involved in receptor degradation of the immature receptor forms. Together, these results demonstrate that the complex-glycosylated receptors are subjected to lysosomal degradation whereas nonglycosylated and core-glycosylated receptor proteins are degraded by the proteasome. Thus, the ERGIC seems to be the last compartment in the secretory pathway that excludes membrane proteins from lysosomal degradation.

Wild-Type V2R and NDI-Causing Mutants Are Polyubiquitinylated. Mature forms of the mutant G201D and wild-type V2R were degraded in lysosomes. In contrast, the immature forms of the wild-type and mutant V2Rs were stabilized when proteasomal activity was blocked, demon-

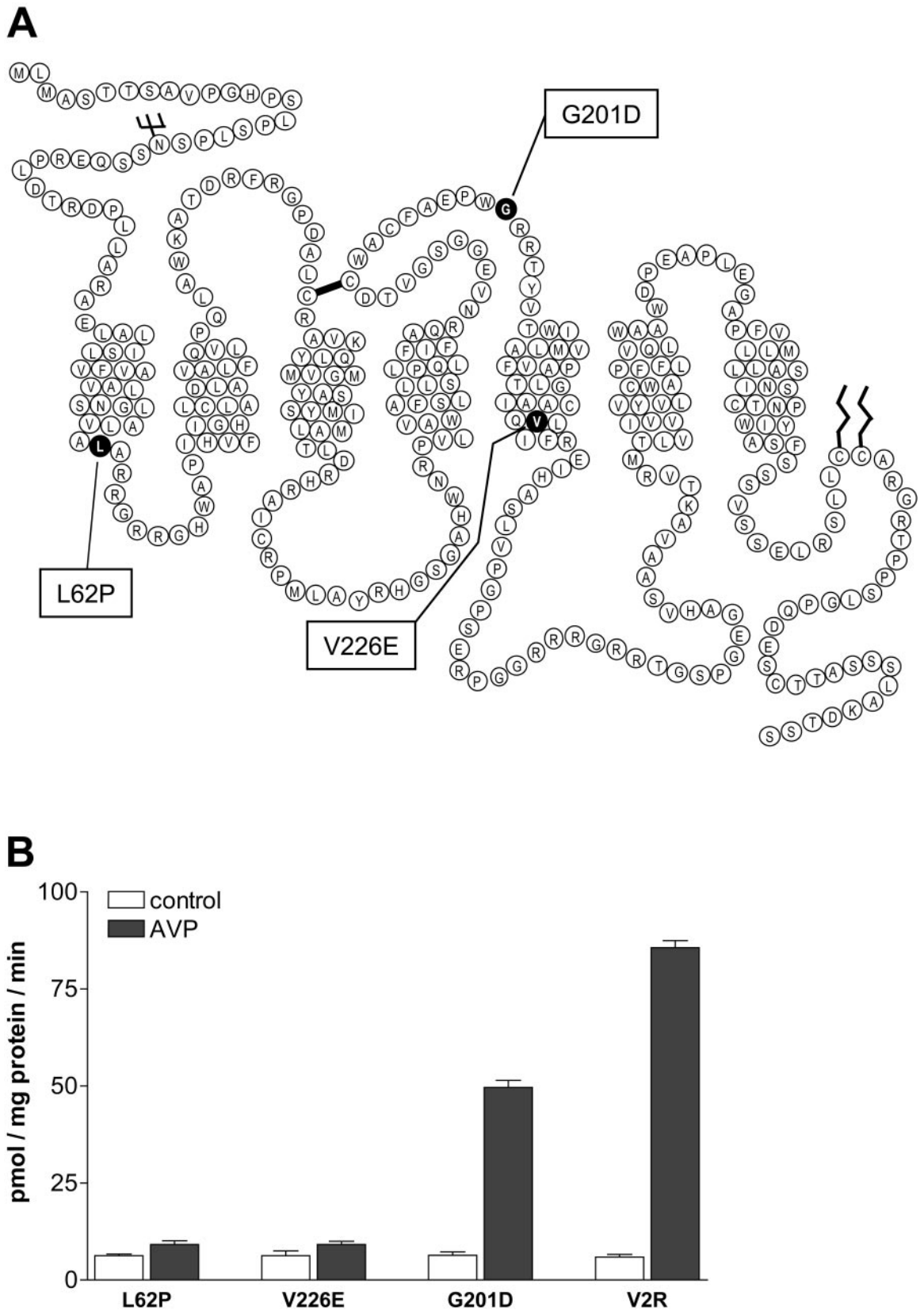

Fig. 1. A, two-dimensional model of the V2R and three NDI-causing mutants. The amino acid sequence of the receptor is shown in one-letter code; *N*-glycosylation at position Asn22, disulfide bond between Cys112 and Cys192, and palmitoylation of residues Cys341 and Cys342 are depicted. Substituted amino acids of mutants L62P, V226E, and G201D are shown in black. B, adenylyl cyclase activity assay with crude membranes of stably transfected HEK293 cells expressing the FLAG-tagged wild-type and mutant V2Rs. Crude membranes were stimulated with 100 nM AVP; controls were performed in the absence of AVP. Data represent mean values of three independent experiments each performed in triplicate. Triplicates differed by less than 10%. S.E.M. values are depicted.

strating a participation of the proteasome in their degradation. ERAD substrates are usually polyubiquitinylated and retrotranslocated from the ER to the cytosol for proteasomal degradation. We investigated whether the NDI-causing mutants and the wild-type V2R are polyubiquitinylated and degraded via the ERAD. FLAG-tagged receptors were precipitated with an α-FLAG M2 affinity gel, and ubiquitinylated receptor proteins were identified with a monoclonal α-polyubiquitin antibody. An immunoreactive smear starting at 250 kDa was only detected in samples that contained receptor constructs (Fig. 5A). MG 132 treatment increased the intensity of this smear, which ranged from 250 to 60 kDa, because of ubiquitin chains of different length. The wild-type V2R and intracellular retained mutants were polyubiquitinylated, indicating that they are suitable substrates for ERAD.

Furthermore, the precipitation efficiency and expression levels of the V2R constructs used for the immunoprecipitations were analyzed by Western blot. No major difference in the expression of FLAG-tagged constructs could be detected between cell clones subjected to immunoprecipitation (Fig. 5B). As expected, for the V2R wild-type and mutant G201D all three receptor forms, the nonglycosylated, core-glycosylated (immature), and complex-glycosylated form, could be detected after MG 132 treatment (compare Supplemental Fig. 3 with Fig. 4, right). Mutants V226E and L62P showed only immature receptor forms. Bands with an apparent molecular mass of ~160 and 80 kDa are presumably multimers of immature receptor proteins (Fig. 5B, *). The apparent smear detected between 200 and 80 kDa represents polyubiquitinylated forms of the V2R.

Wild-Type V2R and NDI-Causing Mutants Interact with ERAD Components. If the immature wild-type V2R and its mutants are degraded via the ERAD, canonical ERAD components that interact with polyubiquitinylated proteins should be identified after precipitation of V2Rs from HEK293 cells. Stably transfected cells expressing the FLAG-tagged wild-type V2R were treated with and without MG 132 overnight, and receptors were immunoprecipitated and separated by SDS-PAGE. Corresponding slices from Coomassie-stained gels of MG 132-treated and untreated samples were excised (for details, see Supplemental Fig. 4). Coprecipitated proteins were in-gel digested with trypsin and identified by NanoLC-tandem mass spectrometry. In samples of untreated cells, only the V2R and Ig γ-1 chain of precipitating antibodies were detected. In samples of MG 132-treated cells, several proteins related to cell stress and protein degradation were identified additionally: immunoglobulin heavy chain-binding protein, the 26S proteasome regulatory subunit 7 (Rpt1/S7), the proteasome 26S non-ATPase subunit 2 (Rpn1/S2), elongation factor 1-α1, 90-kDa heat shock protein-α (HSP 90-α/HSP 86) and 90-kDA heat shock protein-β (HSP 90-β/HSP 84) (Table 1). Both identified proteasomal proteins are subunits of the 19S proteasome regulatory complex.

To verify the mass spectrometry results, we first studied the endogenous expression levels of Rpt1/S7 in whole cell lysates from stable cell clones. A specific immunoreactive band running at 48 kDa was identified in all lysates (Fig. 6, top); no difference in the expression of Rpt1/S7 could be detected between cell clones. Next, blots of immunoprecipitated samples pretreated with or without MG 132 showed

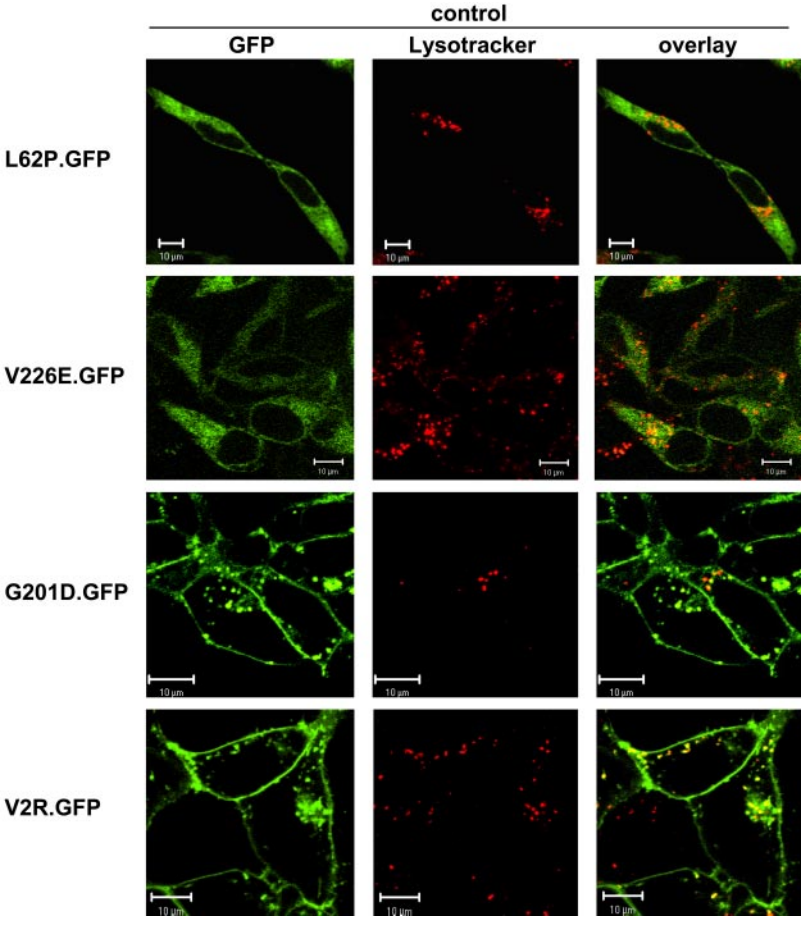

Fig. 2. Lysosomal localization of GFP-tagged wild-type V2R and mutants L62P, V226E, and G201D analyzed in stably expressing living HEK293 cells. Cells were incubated with 150 nM LysoTracker Red for 1 h, and then they were examined by confocal laser-scanning microscopy with horizontal (*xy*) scans. Receptor GFP fluorescence signals are shown in green (left), and LysoTracker Red staining of the same cells is shown in red (middle). GFP and LysoTracker Red fluorescence signals were computer-overlaid (right; overlap is indicated by yellow). The scans show representative cells. Scale bar, 10 μm. Similar data were obtained in five independent experiments.

also a specific band with an apparent mass of 48 kDa, representing Rpt1/S7, and an unspecific band of 60 kDa. In untreated samples of mutant L62P, more Rpt1/S7 could be coprecipitated than in other samples (Fig. 6, middle, Rpt1/S7). As expected, a strong increase in the intensity of the specific immunoreactive band could be observed, when cells were treated with MG 132 (Fig. 6, bottom, Rpt1/S7). As a control for V2R precipitation levels, the same membranes were stripped and used for V2R detection (Fig. 6, V2R). In the presence of MG 132 immature V2R forms were increased, partially explaining the increased coimmunoprecipitation of Rpt1.

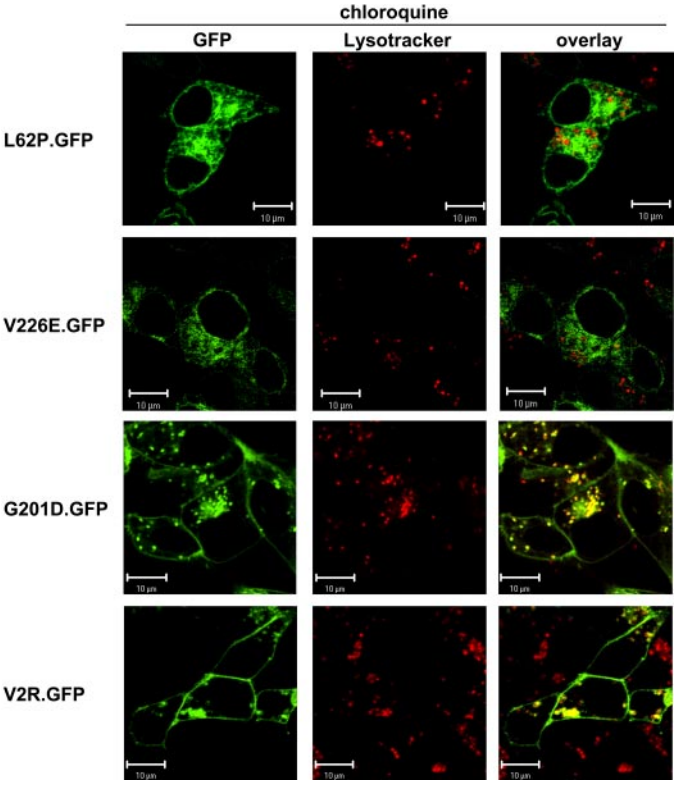

Fig. 3. Inhibition of lysosomal degradation analyzed in living HEK293 cells stably expressing the GFP-tagged wild-type V2R and mutants L62P, V226E, and G201D. Cells were incubated with 100 μM chloroquine for 3 h and with 150 nM LysoTracker Red for 1 h, and then they were examined by confocal laser-scanning microscopy with horizontal (*xy*) scans. Receptor GFP fluorescence signals are shown in green (left), and LysoTracker Red staining of the same cells is shown in red (middle). GFP and LysoTracker Red fluorescence signals were computer-overlaid (right; overlap is indicated by yellow). The scans show representative cells. Scale bar, 10 μm. Similar data were obtained in five independent experiments.

Another canonical ERAD component is p97/VCP, an AAA-ATPase involved in the extraction of misfolded proteins from the ER. It binds to polyubiquitinylated ERAD substrates. Expression levels of p97/VCP were analyzed in whole cell lysates by immunoblotting, and again no differences could be detected between cell clones (Fig. 7, top, p97/VCP). Coimmunoprecipitation studies showed an immunoreactive band with an apparent size of 89 kDa in samples of whole cell lysates detected against p97/VCP. No specific signals were found in coimmunoprecipitated samples from untreated cell clones. The only exception was mutant L62P, where a specific band running at 89 kDa could be identified, indicating an interaction of this mutant with p97/VCP at steady state (Fig. 7, middle, p97/VCP). As expected, treatment with MG 132 increased the amount of coprecipitated p97/VCP significantly (Fig. 7, bottom, p97/VCP). V2R precipitation levels were assayed in the same membranes used for the coimmunoprecipitation study (Fig. 7, V2R).

Similar experiments were also performed with an antibody against Derlin-1, a membrane protein that acts in concert with the p97/VCP to remove dislocation substrate proteins from the ER membrane. A single band with an apparent size of 22 kDa could be identified in samples of whole cell lysates, with no differences in the expression levels between cell clones (Fig. 8A, top, Derlin-1). In immunoprecipitated samples of untreated cells, an immunoreactive band of 22 kDa could be detected with a α-Derlin-1 antibody (data not shown). As expected, the intensity of this band increased, when cells were treated overnight with MG 132 (Fig. 8A, middle, Derlin-1). V2R precipitation levels were verified in the same membranes used for the detection of Derlin-1 (Fig. 8A, bottom, V2R). In addition, we also precipitated Derlin-1 and detected against the

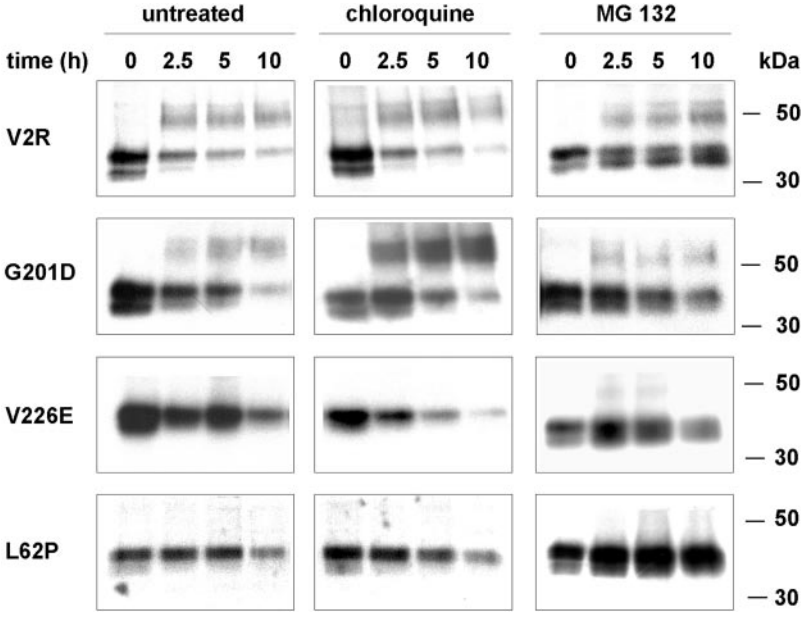

Fig. 4. Degradation of wild-type V2R and NDI-causing mutants in stably expressing HEK293 cells. Cells expressing the FLAG-tagged wild-type V2R and receptor mutants L62P, V226E, and G201D were starved in serum-free DMEM without methionine and cysteine for 16 h, and then they were metabolically labeled with 220 μCi of [^{35}S]-EasyTag protein labeling mix for 45 min without (left) or with 100 μM chloroquine (middle) or 40 μM MG 132 (right). The metabolic labeling was stopped, and at time points 0, 2.5, 5, and 10 h, the cells were harvested, lysed, and immunoprecipitated as described under *Materials and Methods* and separated by SDS-PAGE. The gels were dried and exposed to X-ray film. Molecular mass markers are shown on the right. The results are representative of three independent experiments.

V2R with a mouse monoclonal α-FLAG M2 antibody. As expected, only immature forms of all mutants and the wild-type V2R were coprecipitated by Derlin-1 in a MG 132-dependent manner (Fig. 8B). Unfortunately, reverse coimmunoprecipitation studies were not successful using α-Rpt1 and α-p97/VCP antibodies for precipitation.

Proteasomal inhibition leads to an accumulation of immature, polyubiquitinylated, and nonpolyubiquitinylated proteins, thereby increasing the amount of immunoprecipitated receptors and coprecipitated proteins, in Rpt1/S7, p97/VCP, and Derlin-1, confirming that these proteins bind polyubiquitinylated ERAD substrates (Wang et al., 2004) (Figs. 5, A and B, and 6–8, V2R). Our results show that immature and/or polyubiquitinylated V2Rs interact with ERAD components, namely, Rpt1/S7, p97/VCP, and Derlin-1. However, these results do not preclude the possibility that other ERAD proteins participate in this complex.

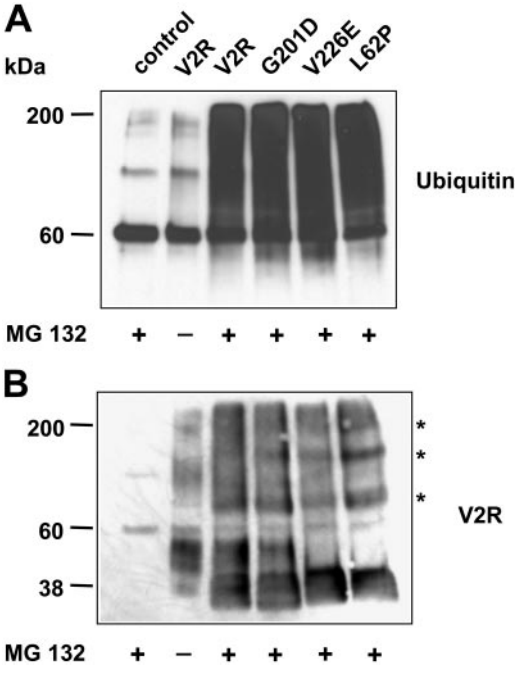

Fig. 5. Ubiquitinylation and immunoprecipitation of FLAG-tagged V2R receptor constructs. A, immunoprecipitation of polyubiquitinylated receptors. HEK293 cells stably expressing wild-type and mutant V2Rs were treated with 20 μM MG 132 for 16 h (+) or left untreated (−). Proteins eluted from α-FLAG M2 affinity gel were analyzed by SDS-PAGE and Western blot analysis with a monoclonal mouse α-polyubiquitin antibody and a POD-conjugated α-mouse antibody. B, stably expressing HEK293 cells were lysed, and receptors were immunoprecipitated with an α-FLAG M2 affinity gel as described in A. Receptors were detected with a mouse monoclonal α-FLAG M2 antibody, a POD-conjugated α-mouse antibody, and the ECL system. Control, untransfected HEK293 cells. The asterisk (*) indicates presumed V2R multimers. Data are representative of six independent experiments.

Immature Receptor Proteins Are Retrotranslocated into the Cytosol. V2R mutants are polyubiquitinylated and interact with membrane and cytosolic components of the ERAD complex. For determination of the site of turnover, cytosolic and membrane fractions of HEK293 cells stably expressing FLAG-tagged L62P mutants and wild-type receptors were isolated. Immunoblot analysis revealed specific bands in the cytosolic and membrane fractions of MG 132-treated cells (Fig. 9). In the cytosolic fraction of L62P, a specific band of approximately 35-kDa could be detected that corresponds to the unglycosylated receptor form. In the membrane fraction, a specific band of 38 kDa could be identified, representing the core-glycosylated receptor form. For the wild-type receptor, a similar band pattern could be recognized; however, in the membrane fraction of MG 132-treated cells, two additional immunoreactive bands could be detected, one band between 53 and 45 kDa and a second band of 35 kDa. These bands represent the complex- and unglycosylated receptor forms, respectively. As expected, an increase in the intensity or emergence of bands representing the immature receptor forms was observed in cells treated with MG 132, confirming our results obtained by pulse-chase analysis. These results indicate that ERAD substrates are deglycosylated and retrotranslocated completely into the cytosol. Furthermore, glycosylated receptor forms are restricted to the membrane fraction.

Taken together, our results demonstrate that core-glycosylated disease-causing mutants of the V2R are retrotranslocated, deglycosylated, and degraded via a Derlin-1- and p97/VCP mediated ERAD pathway. This degradation pathway is independent of the location of the misfolded domain within the V2R.

Discussion

Two major pathways may operate in the cell to degrade intracellularly retained GPCRs: the ubiquitin-dependent proteasomal pathway and the lysosomal pathway (Ciechanover, 2006). It is accepted that integral membrane proteins expressed at the cell surface are internalized and degraded

TABLE 1

V2R-associated proteins identified by NanoLC-electrospray ionization-MS/MS in the presence of MG 132

V2Rs were immunoprecipitated via their FLAG tag, and they were separated by SDS-PAGE. Coprecipitated proteins were stained with Coomassie Blue, excised from the gel, and subjected to in-gel digestion by trypsin. The NanoLC-MS/MS experiments were performed, and peptides were identified in a data-dependent mode (survey scanning) using one MS scan followed by MS/MS scans of the most abundant peak. The most abundant proteins identified are shown. Proteins listed were not found in cells that were not treated with MG132 (with the exception of the V2R and Ig γ-1 chain C region). The complete set of proteins identified in the absence and presence of MG132 is available in Supplemental Tables 1 and 2.

Protein	SwissProt	Molecular Mass	Score	Peptides (MS/MS)
		Da		
Immunoglobulin heavy chain-binding protein	P11021	72,288	1399	23
Rpt1/S7	P35998	48,472	352	5
Rpn1/S2	Q13200	100,136	447	9
Elongation factor 1-α1	P68104	50,109	621	13
HSP 90-β/HSP 84	P08238	83,081	390	8
HSP 90-α/HSP 86	P07900	84,476	253	5
V2R	P30518	40,253	246	5
Mouse Ig γ-1 chain C region	P01869	43,359	206	4

by the lysosome. In contrast, membrane proteins retained in the ER by the quality control system are retrotranslocated into the cytosol, and they are degraded by the ubiquitin/proteasome system. This particular degradation pathway is known as ERAD (Brodsky and McCracken, 1999; Hampton, 2002). In mammalian cells, the ERAD pathway is still not well characterized. In addition, the degradation pathways used by the cell when proteins are retained outside the ER are also not well defined.

In the present study, we analyzed the degradation pathways of the wild-type V2R and three intracellularly retained disease-causing mutants. These particular mutants are good

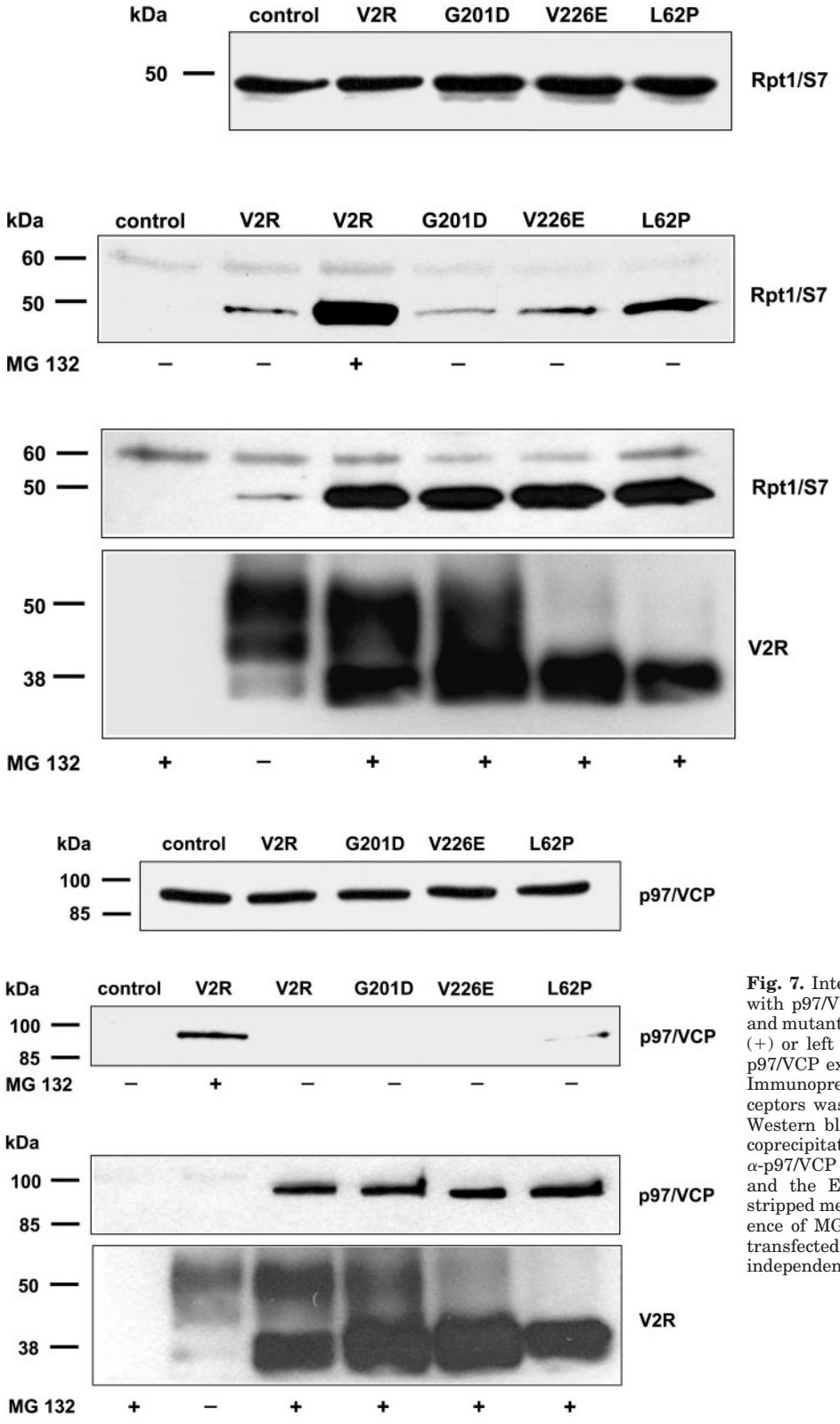

Fig. 6. Total cell lysates analyzed for Rpt1/S7 expression by Western blotting (top). HEK293 cells stably expressing wild-type and mutant V2Rs were treated with 20 μM MG 132 for 16 h (+) or left untreated (−). Immunoprecipitation of FLAG-tagged V2R wild-type and mutant receptors was performed, and receptors were analyzed by immunoblotting in the two middle panels. Detection of coprecipitated subunits of the 26S proteasome was done with a polyclonal rabbit α-Rpt1/S7 antibody and a POD-conjugated α-rabbit antibody. V2R precipitation levels of the stripped membrane used for Rpt1 detection in the presence of MG 132 are shown (bottom). Controls were nontransfected HEK293 cells. Data are representative of four independent experiments.

Fig. 7. Interaction of the V2R and NDI-causing mutants with p97/VCP. HEK293 cells stably expressing wild-type and mutant V2Rs were treated with 20 μM MG 132 for 16 h (+) or left untreated (−). Total cell lysates analyzed for p97/VCP expression by Western blotting are shown (top). Immunoprecipitation of the V2R wild-type and mutant receptors was carried out, and receptors were analyzed by Western blotting in the two middle panels. Detection of coprecipitated p97/VCP was done with a polyclonal rabbit α-p97/VCP antibody, POD-conjugated α-rabbit antibody, and the ECL system. V2R precipitation levels of the stripped membrane used for p97/VCP detection in the presence of MG 132 are shown (bottom). Controls were nontransfected HEK293 cells. Data are representative of four independent experiments.

tools to analyze the degradation pathways, because they are retained in different compartments of the secretory pathway (Hermosilla et al., 2004). Furthermore, the defects resulting from mutations are localized in different domains of the protein; L62P is located in a cytosolic domain (beginning of the first intracellular loop), G201D is in a luminal domain (second extracellular loop), and V226E is in a transmembrane domain (fifth helix) (Fig. 1A). The colocalization studies in living cells showed that the wild-type V2R and mutant G201D are localized in lysosomes. Furthermore, pulse-chase experiments demonstrated that the complex glycosylated (mature) forms of mutant G201D are degraded by lysosomes. Similar results have been reported for the wild-type V2R and mature mutants at steady state and after activation by AVP (Robben et al., 2004). Our results demonstrate that membrane proteins, which reach the Golgi apparatus or are expressed at the plasma membrane, are transported to the lysosomal compartment for degradation at steady state. However, it is not known whether receptors that reach the Golgi apparatus are first transported to the plasma membrane and then to lysosomes, or whether a direct route is followed, or whether both routes are operating.

All immature V2R forms (mutant and wild type) were degraded via the ERAD, regardless of their intracellular localization (Figs. 6–8, Supplemental Fig. 2). As expected, all mutants were found to be polyubiquitinylated (Fig. 5, A and B). We could demonstrate that in the presence of a proteasome inhibitor, all nonglycosylated and core-glycosylated V2R proteins were stabilized (Figs. 4, MG 132, and 5B), and that wild-type and mutant receptors coprecipitated Derlin-1, p97/VCP, Rpt1/S7, and Rpn2/S2. These results indicate that newly synthesized misfolded or unfolded receptors are targeted to the ERAD by the quality control system. Therefore, we conclude that the ERAD is predominantly involved in the degradation of immature disease-causing V2R mutants, but it is also involved in the degradation of immature, misfolded wild-type V2Rs. The fact that immature wild-type proteins also are degraded by the ERAD has been described for the δ opioid (Petäjä-Repo et al., 2001), luteinizing hormone receptor (Pietilä et al., 2005), and the cystic fibrosis transmembrane regulator, and it is ascribed to inefficient folding or structural instability of the proteins (Sun et al., 2006). Presented data show that only nonglycosylated and core-glycosylated misfolded receptor proteins are degraded via ERAD and that complex-glycosylated misfolded receptor proteins are targeted to lysosomal degradation. Our results demonstrate that the ERGIC is the last compartment of quality control that participates in ERAD.

The wild-type V2R has been described to be ubiquitinylated together with β-arrestin 2, but only after agonist-induced internalization; both proteins are thought to be transported together to the lysosomal compartment for degradation (Martin et al., 2003). The ubiquitin ligases involved in the polyubiquitinylation of immature wild-type V2Rs and NDI-causing mutants are still unknown. Most probable ubiquitin ligases such as gp78/autocrine motility factor receptor (membrane-associated E3), Hrd1 (membrane-associated E3), and Ufd2 (E4 enzyme), which interact with p97/VCP and participate in the retrotranslocation of ERAD substrates (Ye, 2006), are involved in the polyubiquitinylation of immature forms of the V2R. In an attempt to determine the E3 that is responsible for the polyubiquitinylation of NDI-causing V2R mutants, immunoprecipitated samples were analyzed for the presence of Hrd1. It was not possible for us to specifically detect Hrd1 in these samples (data not shown).

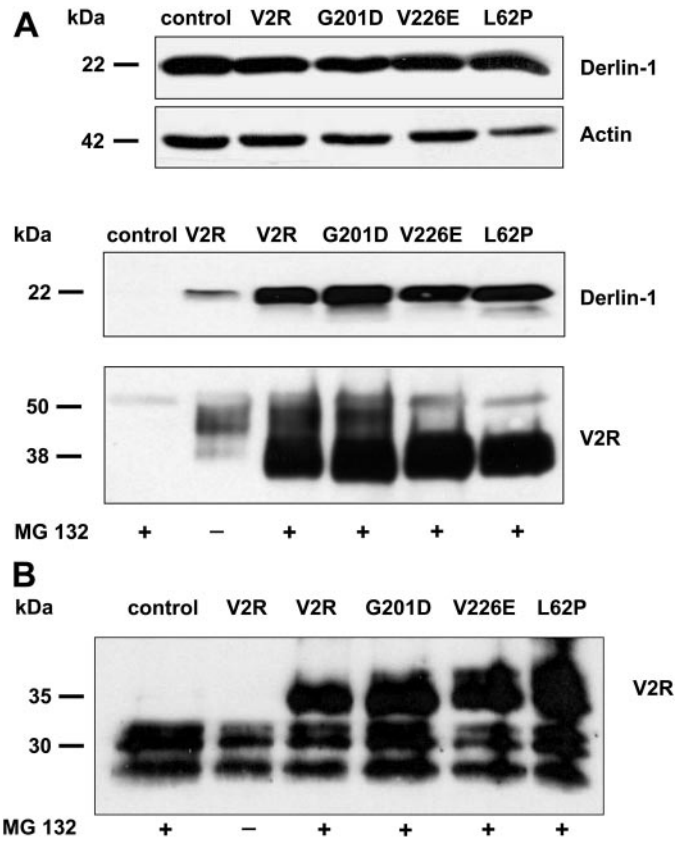

Fig. 8. Interaction of the V2R and NDI-causing mutants with Derlin-1. A, HEK293 cells stably expressing wild-type and mutant V2Rs were treated with 20 μM MG 132 for 16 h (+) or left untreated (−). Total cell lysates of untreated cells analyzed for Derlin-1 expression by Western blotting are shown (top). Actin was used as loading control. Immunoprecipitation of the wild-type V2R and mutant receptors was carried out as described under *Materials and Methods*, and receptors were analyzed by Western blotting. Detection of coprecipitated Derlin-1 was done with a polyclonal rabbit α-Derlin-1 antibody, POD-conjugated α-rabbit antibody, and the ECL system. V2R precipitation levels of the stripped membrane used for Derlin-1 detection in the presence of MG 132 are shown (bottom). Controls were nontransfected HEK293 cells. B, coimmunoprecipitation study of the interaction between Derlin-1 and the V2R and its disease-causing mutants. Precipitations were done with a polyclonal α-Derlin-1 antibody (Santa Cruz Biotechnology, Inc.), and detection was performed with a monoclonal α-FLAG M2 antibody. Specific bands, representing the immature forms of the V2R, could only be detected in the presence of MG 132. Controls were nontransfected HEK293 cells. Data are representative of four independent experiments.

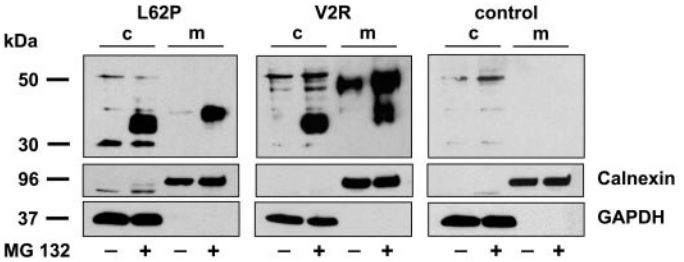

Fig. 9. Cellular fractions analyzed for V2R expression. Stably expressing HEK293 cells were either treated with 20 μM MG 132 for 16 h (+) or left untreated (−). Isolated cytosolic (c) and membrane (m) fractions were analyzed by SDS-PAGE and immunoblotting. Detection of FLAG-tagged V2R constructs was done with a mouse monoclonal α-FLAG M2 antibody and a POD-conjugated α-mouse antibody. Controls were nontransfected HEK293 cells (control). The purity of cell fractions was confirmed by the detection of calnexin and GAPDH in all isolated fractions. Data are representative of three independent experiments.

In yeast, three distinct ERAD pathways have been proposed: ERAD-L, ERAD-M, and ERAD-C, which destroy proteins with misfolded luminal, intramembrane, and cytosolic domains, respectively (Carvalho et al., 2006). These pathways use the cytosolic Cdc48 ATPase complex, whose membrane recruitment is facilitated by Ubx2. However, the ERAD-L and ERAD-M pathway require the ubiquitin ligase Hrd1, additionally ERAD-L needs Der1; both proteins have mammalian homologs (Hrd1, gp78, and Derlin-1, -2, and -3) that are involved in the mammalian ERAD. ERAD-C requires the ubiquitin ligase Doa10, but not Hrd1 and Der1. Our results for the studied V2R mutants suggest that only the Derlin-1-mediated ERAD pathway is used in HEK293 cells. Regardless of their misfolded domain, either cytosolic (L62P), luminal (G201D), or membrane (V226E), all mutants precipitated Derlin-1 and p97/VCP, the mammal homolog of Cdc48. We also investigated a second mutant with a mutation within the fourth transmembrane domain (S167L) that also interacts with Derlin-1 (data not shown). Our results demonstrate that at least the putative channel protein Derlin-1 and the AAA-ATPase p97/VCP are central components of the retrotranslocation machinery of the ERAD in a mammalian system.

Sec61α and Derlin-1 (and its homologs Derlin-2 and -3) are thought to be the channel or to be located at the site of retrotranslocation of misfolded proteins from the ER to the cytosol (Ye et al., 2004, 2005; Kalies et al., 2005). It is still unclear whether the proteasome is recruited to the ER membrane by binding to the retrotranslocation channel, so that substrates are directly released into the proteasome (Kalies et al., 2005); or whether substrates are first released into the cytosol and then targeted to the proteasome (Petäjä-Repo et al., 2001; Meusser et al., 2005). It has been shown that the 26S proteasome disassembles in an ATP-dependent catalytic cycle, leading to 19S RP subcomplexes and free 26S protease regulatory subunit 5a (Babbitt et al., 2005). In contrast, 19S RPs are able to interact with Sec61 at the ER membrane (Ng et al., 2007). Wahlman et al. (2007) demonstrated that ATP, the 19S RP, the ER luminal chaperone PDI, and Derlin-1 are sufficient to retrotranslocate a soluble ERAD substrate in vitro (Wahlman et al., 2007). It is noteworthy that retrotranslocation of the substrate was ubiquitin, Sec61α, p97/VCP, and Ufd1 and Npl4 cofactors independent. However, the ERAD substrate used in this study was the fluorescence-labeled Δgpαf, a soluble, nonubiquitinylated protein lacking disulfide bonds and transmembrane domains, which is derivative of the yeast pro-α factor mating pheromone. In our system, V2Rs were located in the ER-membrane, glycosylated, and/or polyubiquitinylated, which might explain the differences regarding the association with p97/VCP. Furthermore, we could identify deglycosylated V2R (wild type and mutant) in the cytosolic fraction after proteasomal inhibition, indicating a complete retrotranslocation of the receptors to the cytosol. Our results support the idea that 19S RP plays a central role in retrotranslocation and recognition of ERAD substrates, before their degradation by the 26S proteasome. Because retrotranslocated V2Rs seemed not to be polyubiquitinylated, the interaction with 19S RP might induce their deubiquitinylation. Therefore, we propose that subunits of the 19S RP, like Rpt1/S7, Rpn1/S2, and 26S protease regulatory subunit 5a, function as scaffolds on the ER-substrate for the 19S RP and 20S core particle, facilitating the assembly of the 26S proteasome at the substrate. Moreover, Derlin-1 is centrally implicated in the recognition, retrotranslocation, or both of the V2R, independent of the location of the misfolded domain.

Until now, no effective pharmacological treatment of NDI has been developed. A promising therapeutic strategy is the use of pharmacochaperones that rescue transport-defective receptors from the early secretory pathway to the plasma membrane (Wüller et al., 2004; Bernier et al., 2006). Another possible approach to rescue intracellularly retained proteins may be the inhibition of the ERAD, as exemplary shown for the CFTR by reducing the expression of p97/VCP or blocking the proteasome with bortezomib (Vij et al., 2006). However, this new therapeutic strategy may be only valid for NDI-causing mutants that are transport-defective but still functional.

In summary, our data reveal that the quality control system of the cell determines the degradation pathway of NDI-causing mutants of the V2R. Immature receptor proteins that reach the ERGIC are polyubiquitinylated and degraded via the ERAD; all other mature receptor proteins located beyond the ERGIC are degraded via lysosomes. Furthermore, we demonstrate that a Derlin-1- and p97/VCP-mediated ERAD pathway is responsible for the degradation of the V2R and its disease-causing mutants, regardless of the location of the misfolded domain within the receptor.

Acknowledgments

We thank Ursula Brandt, Stefanie Schneider, and Michael Schümann for excellent technical work; Philipp Voigt for technical advice; and Ralf Schülein, Márta Szaszák, and Evelina Grantcharova for critical reading of the manuscript and helpful discussions.

References

Aridor M and Hannan LA (2000) Traffic jam: a compendium of human diseases that affect intracellular transport processes. *Traffic* **1:**836–851.
Aridor M and Hannan LA (2002) Traffic jams II: an update of diseases of intracellular transport. *Traffic* **3:**781–790.
Babbitt SE, Kiss A, Deffenbaugh AE, Chang YH, Bailly E, Erdjument-Bromage H, Tempst P, Buranda T, Sklar LA, Baumler J, et al. (2005) ATP hydrolysis-dependent disassembly of the 26S proteasome is part of the catalytic cycle. *Cell* **121:**553–565.
Bernier V, Morello JP, Zarruk A, Debrand N, Salahpour A, Lonergan M, Arthus MF, Laperrière A, Brouard R, Bouvier M, et al. (2006) Pharmacologic chaperones as a potential treatment for X-linked nephrogenic diabetes insipidus. *J Am Soc Nephrol* **17:**232–243.
Bouley R, Lin HY, Raychowdhury MK, Marshansky V, Brown D, and Ausiello DA (2005) Downregulation of the vasopressin type 2 receptor after vasopressin-induced internalization: involvement of a lysosomal degradation pathway. *Am J Physiol Cell Physiol* **288:**C1390–C1401.
Brodsky JL and McCracken AA (1999) ER protein quality control and proteasome-mediated protein degradation. *Semin Cell Dev Biol* **10:**507–513.
Carvalho P, Goder V, and Rapoport TA (2006) Distinct ubiquitin-ligase complexes define convergent pathways for the degradation of ER proteins. *Cell* **126:**361–373.
Ciechanover A (2006) Intracellular protein degradation: from a vague idea thru the lysosome and the ubiquitin-proteasome system and onto human diseases and drug targeting. *Exp Biol Med (Maywood)* **231:**1197–1211.
Czupalla C, Mansukoski H, Riedl T, Thiel D, Krause E, and Hoflack B (2006) Proteomic analysis of lysosomal acid hydrolases secreted by osteoclasts: implications for lytic enzyme transport and bone metabolism. *Mol Cell Proteomics* **5:**134–143.
Gazit G, Lu J, and Lee AS (1999) De-regulation of GRP stress protein expression in human breast cancer cell lines. *Breast Cancer Res Treat* **54:**135–146.
Hampton RY (2002) ER-associated degradation in protein quality control and cellular regulation. *Curr Opin Cell Biol* **14:**476–482.
Hermosilla R, Oueslati M, Donalies U, Schönenberger E, Krause E, Oksche A, Rosenthal W, and Schülein R (2004) Disease-causing V(2) vasopressin receptors are retained in different compartments of the early secretory pathway. *Traffic* **5:**993–1005.
Kalies KU, Allan S, Sergeyenko T, Kroger H, and Romisch K (2005) The protein translocation channel binds proteasomes to the endoplasmic reticulum membrane. *EMBO J* **24:**2284–2293.
Kopito RR (2000) Aggresomes, inclusion bodies and protein aggregation. *Trends Cell Biol* **10:**524–530.
Krause G, Hermosilla R, Oksche A, Rutz C, Rosenthal W, and Schülein R (2000)

Molecular and conformational features of a transport-relevant domain in the C-terminal tail of the vasopressin V2 receptor. *Mol Pharmacol* **57:**232–242.
Kyhse-Andersen J (1984) Electroblotting of multiple gels: a simple apparatus without buffer tank for rapid transfer of proteins from polyacrylamide to nitrocellulose. *J Biochem Biophys Methods* **10:**203–209.
Martin NP, Lefkowitz RJ, and Shenoy SK (2003) Regulation of V2 vasopressin receptor degradation by agonist-promoted ubiquitination. *J Biol Chem* **278:** 45954–45959.
Meusser B, Hirsch C, Jarosch E, and Sommer T (2005) ERAD: the long road to destruction. *Nat Cell Biol* **7:**766–772.
Ng W, Sergeyenko T, Zeng N, Brown JD, and Romisch K (2007) Characterization of the proteasome interaction with the Sec61 channel in the endoplasmic reticulum. *J Cell Sci* **120:**682–691.
Oksche A, Dehe M, Schülein R, Wiesner B, and Rosenthal W (1998) Folding and cell surface expression of the vasopressin V2 receptor: requirement of the intracellular C-terminus. *FEBS Lett* **424:**57–62.
Petäjä-Repo UE, Hogue M, Laperrière A, Bhalla S, Walker P, and Bouvier M (2001) Newly synthesized human δ opioid receptors retained in the endoplasmic reticulum are retrotranslocated to the cytosol, deglycosylated, ubiquitinated, and degraded by the proteasome. *J Biol Chem* **276:**4416–4423.
Pietilä EM, Tuusa JT, Apaja PM, Aatsinki JT, Hakalahti AE, Rajaniemi HJ, and Petäjä-Repo UE (2005) Inefficient maturation of the rat luteinizing hormone receptor: a putative way to regulate receptor numbers at the cell surface. *J Biol Chem* **280:**26622–26629.
Robben JH, Knoers NV, and Deen PM (2004) Regulation of the vasopressin V2 receptor by vasopressin in polarized renal collecting duct cells. *Mol Biol Cell* **15:**5693–5699.
Robben JH, Knoers NV, and Deen PM (2005) Characterization of vasopressin V2 receptor mutants in nephrogenic diabetes insipidus in a polarized cell model. *Am J Physiol Renal Physiol* **289:**F265–F272.
Robben JH, Knoers NV, and Deen PM (2006) Cell biological aspects of the vasopressin type-2 receptor and aquaporin 2 water channel in nephrogenic diabetes insipidus. *Am J Physiol Renal Physiol* **291:**F257–F270.
Sambrook J and Russell DW (2001) *Molecular Cloning: A Laboratory Manual*, Cold Spring Harbor Laboratory Press, Cold Spring Harbor, NY.
Schülein R, Hermosilla R, Oksche A, Dehe M, Wiesner B, Krause G, and Rosenthal W (1998) A dileucine sequence and an upstream glutamate residue in the intracellular carboxyl terminus of the vasopressin V2 receptor are essential for cell surface transport in COS.M6 cells. *Mol Pharmacol* **54:**525–535.
Schülein R, Liebenhoff U, Müller H, Birnbaumer M, and Rosenthal W (1996) Properties of the human arginine vasopressin V2 receptor after site-directed mutagenesis of its putative palmitoylation site. *Biochem J* **313:**611–616.
Sun F, Zhang R, Gong X, Geng X, Drain PF, and Frizzell RA (2006) Derlin-1 promotes the efficient degradation of the cystic fibrosis transmembrane conductance regulator (CFTR) and CFTR folding mutants. *J Biol Chem* **281:**36856–36863.
Vij N, Fang S, and Zeitlin PL (2006) Selective inhibition of endoplasmic reticulum-associated degradation rescues ΔF508-cystic fibrosis transmembrane regulator and suppresses interleukin-8 levels: therapeutic implications. *J Biol Chem* **281:** 17369–17378.
Wahlman J, Demartino GN, Skach WR, Bulleid NJ, Brodsky JL, and Johnson AE (2007) Real-time fluorescence detection of ERAD substrate retrotranslocation in a mammalian in vitro system. *Cell* **129:**943–955.
Wang Q, Song C, and Li CC (2004) Molecular perspectives on p97-VCP: progress in understanding its structure and diverse biological functions. *J Struct Biol* **146:** 44–57.
Werner ED, Brodsky JL, and McCracken AA (1996) Proteasome-dependent endoplasmic reticulum-associated protein degradation: An unconventional route to a familiar fate. *Proc Natl Acad Sci U S A* **93:**13797–13801.
Wüller S, Wiesner B, Löffler A, Furkert J, Krause G, Hermosilla R, Schaefer M, Schülein R, Rosenthal W, and Oksche A (2004) Pharmacochaperones post-translationally enhance cell surface expression by increasing conformational stability of wild-type and mutant vasopressin V2 receptors. *J Biol Chem* **279:**47254–47263.
Ye Y (2006) Diverse functions with a common regulator: ubiquitin takes command of an AAA ATPase. *J Struct Biol* **156:**29–40.
Ye Y, Shibata Y, Kikkert M, van Voorden S, Wiertz E, and Rapoport TA (2005) Inaugural Article: Recruitment of the p97 ATPase and ubiquitin ligases to the site of retrotranslocation at the endoplasmic reticulum membrane. *Proc Natl Acad Sci U S A* **102:**14132–14138.
Ye Y, Shibata Y, Yun C, Ron D, and Rapoport TA (2004) A membrane protein complex mediates retro-translocation from the ER lumen into the cytosol. *Nature* **429:**841–847.
Zhang K and Kaufman RJ (2006) The unfolded protein response: a stress signaling pathway critical for health and disease. *Neurology* **66:**S102–S109.

Address correspondence to: Dr. Ricardo Hermosilla, Leibniz-Institut für Molekulare Pharmakologie (FMP), Campus Buch, Robert-Rössle Str. 10, 13125 Berlin, Germany. E-mail: ricardo.hermosilla@charite.de